JCTC Journal of Chemical Theory and Computation

Direct Dynamics Studies on the Hydrogen Abstraction Reactions of an F Atom with CH_3X (X = F, Cl, and Br)

Li Wang, Jing-yao Liu, Ze-sheng Li,* and Chia-chung Sun

Institute of Theoretical Chemistry, State Key Laboratory of Theoretical and Computational Chemistry, Jilin University, Changchun 130023, P. R. China

Received September 26, 2004

Abstract: The hydrogen abstraction reactions of F + CH_3F (R1), F + CH_3Cl (R2), and F + CH_3Br (R3) are investigated by the dual-level direct dynamics method. Optimized geometries and frequencies of all the stationary points and extra points along the minimum-energy path (MEP) are obtained at the MP2/6-311G(d, p) level of theory, and then the energy profiles are refined at the CCSD(T)/6-311++G(3df, 2pd) level of theory. The basis set superposition error (BSSE) on the energy changes is corrected by means of the counterpoise method. Using the variational transition state theory (VTST) with the inclusion of the small-curvature tunneling correction, the rate constants are calculated over a wide temperature range of 189−2000 K. It is found that the activation energies for the title reactions are on the order of R1 > R2 > R3 and the rate constants exhibit just the opposite order of $k_3 > k_2 > k_1$. Both the activation energies and the rate constants show the clear-cut linear correlations with the hardness η of the halomethane molecules. Good agreement between the calculated and experimental rate constants is obtained at the measured temperatures. Furthermore, we hope that the theoretical studies for these compounds can give further information concerning the effects of halogen substitution on the rate constants of this class of hydrogen abstraction reactions.

Introduction

The adverse effect of halogen-substituted hydrocarbons has attracted international attention.[1−3] The important atmospheric species, halomethanes, should be responsible for the depletion of the ozone layer in the stratosphere and the greenhouse effect. Thus, to estimate the atmospheric lifetimes of such species, accurate data for the rate constants as well as their temperature dependencies are needed. The reactions including fluorine atoms attract lots of attentions because fluorine atoms can react with most trace atmospheric compounds with the rapid rate constants. In early literature, the considerable experimental investigations[4−10] have been devoted to the kinetics of the hydrogen abstraction reactions of F + CH_3X (X=F, Cl, and Br). For the reaction F + CH_3F → HF + CH_2F (R1), there is larger discrepancy among the measured rate constants. The experimented value of (6.59 ± 1.51) × 10^{-12} cm^3 $molecule^{-1}$ s^{-1} [10] is much lower than that of 8.8 × 10^{-11} cm^3 $molecule^{-1}$ s^{-1}.[4] Very recently, Persky determined the rate constant of (2.8 ± 0.2) × 10^{-11} cm^3 $molecule^{-1}$ s^{-1} at 298 K,[9] which agrees well with other measured values. However, almost all the studies are carried out at room temperature except that Persky[9] reported the temperature dependence of rate constants from 189 to 298 K and the Arrhenius expression is given. With respect to the reaction F + CH_3Cl → HF + CH_2Cl (R2), there are three experimental values available at 295 or 298 K,[7,11−12] which show well mutual consistency. Also some experiments are conducted on the reaction of F + CH_3Br → HF + CH_2Br (R3), in which the results determined by Iyer and Rowland[13] are somewhat higher than other values.[7,14−15] Contrary to the considerable experiments, no theoretical information is available on the reactions of F atoms with halomethanes.

Here, a dual-level (X//Y)[16−18] direct dynamics method is applied to study the kinetic nature of the reactions over a wide temperature range. In this approach, the required electronic structure information for the stationary points and a series of extra points along the minimum energy path

* Corresponding author fax: +86−431−8498026; e-mail: ljy121@mail.jlu.edu.cn, liujy121@163.com.

10.1021/ct049932+ CCC: $30.25
Published on Web 01/29/2005

(MEP) are obtained directly from ab initio calculations. Subsequently, by means of the Polyrate 8.4.1 program[19] the rate constants are carried out using the variational transition state theory (VTST)[20,21] proposed by Truhlar and co-workers for each reaction. The comparison between theory and experiment is discussed. Due to lack of the temperature dependence kinetic data of these reactions, the present theoretical results are expected to be useful and reasonable to estimate the dynamical properties of these reactions over a wide temperature range where no experimental value is available.

Calculation Methods

All of the electronic structure calculations are carried out with the Gaussian 98 program.[22] The geometries, energies, and frequencies of all the stationary points, including the reactants, transition states (TSs), and products involved in the three reactions, are computed by using restricted or unrestricted second-order Møller−Plesset perturbation theory with the 6-311G(d, p) basis set (MP2/6-311G(d, p)). To obtain more reliable reaction enthalpies and barrier heights, high level single-point calculations for the stationary points are performed at the CCSD(T) level (coupled-cluster approach with single and double substitutions including a perturbative estimate of connected triples substitutions) with the flexible 6-311++G(3df, 2pd) basis set using the MP2 optimized geometries. To test the consistency of the calculated geometries and energies, we also employ higher electronic correlation level QCISD (quadratic configuration interaction with single and double substitutions) for the $CH_3F + F$ reaction. The minimum-energy path (MEP) is calculated by the intrinsic reaction coordinate (IRC) theory at the MP2 level to confirm that the TS really connects with minima along the reaction path. The first and second energy derivatives at geometries along the MEP are obtained to calculate the curvature of the reaction path and to calculate the generalized vibrational frequencies along the reaction path. The potential profile is further refined at the CCSD(T)/6-311++G(3df, 2pd)//MP2/6-311G(d, p) level. Furthermore, the effect of the basis set superposition error on the energies is considered by means of the counterpoise method proposed by Boys and Bernardi.[23] The initial information on the potential energy surface is used to evaluate the rate constants by means of the Polyrate 8.4.1 program. The rate constants are calculated by using the variational transition state theory (VTST)[20,21] proposed by Truhlar and co-workers. The specific level of VTST that we used is canonical variational transition-state theory (CVT)[24] with the small-curvature tunneling (SCT)[25] method. The $^2P_{1/2}$ and $^2P_{3/2}$ electronic states of the fluorine atom, with a splitting of $\Delta E = 404$ cm^{-1} (1.15 kcal mol^{-1}) due to the spin−orbit coupling, are used in the calculation of the electronic partition functions. It should be noted that the spin−orbit effect would lower the energy of the lower state (i.e., $^2P_{3/2}$ electronic state) of the F atom. Furthermore, as pointed out by Truhlar et. al.,[26] the spin−orbit coupling is essentially fully quenched at the transition state and the nonrelativistic treatment will give a good approximation to the correct energy. With the same consideration, in this article the effect of the spin−orbit coupling is considered in the reactant partition function and is neglected in the saddle point, that is, the effective barrier heights are increased. As a result, the rate constants can be expected to slightly decrease when the spin−orbit coupling is considered only in the reactant partition function. The curvature components are calculated by using a quadratic fit to obtain the derivative of the gradient with respect to the reaction coordinate.

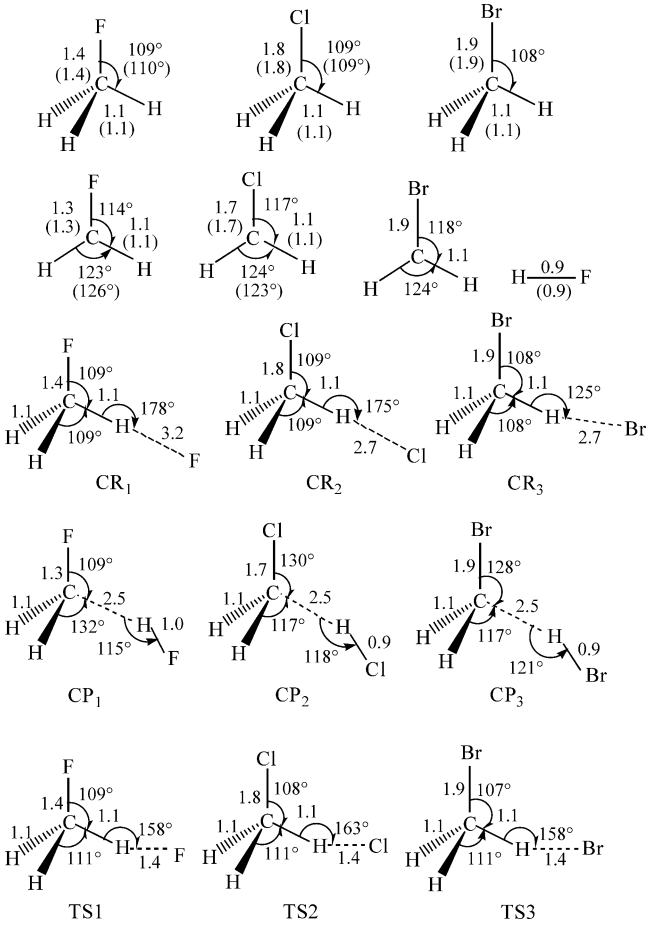

Figure 1. Optimized geometries of CH_3F, CH_3Cl, CH_3Br, HF, CH_2F, CH_2Cl, CH_2Br, complexes, and three transition states at the MP2/6-311G(d, p) level. The values in the parentheses are the experimental values.[27−29] Bond lengths are in angstroms and angles are in degrees.

Results and Discussion

1. Stationary Points. The geometric parameters of all the stationary points including the reactants, complexes, products, and transition states optimized at the MP2/6-311G(d, p) level are shown in Figure 1 as well as the available experimental values[27−29] for comparison. As can be seen from Figure 1, the largest deviation between theoretical bond lengths and experimental values is 0.1 Å, and the largest deviation of the angle is about 3°. It is clear that the theoretical values are in reasonable accord with the experimental ones. At the MP2 level, complexes CR_1, CR_2, and CR_3 are located at the entrance channel of reactions R1, R2, and R3, respectively, in which the H−F bond lengths are 3.2, 2.7, and 2.7 Å, respectively. Also, there exist three complexes CP_1, CP_2, and CP_3 located at the product sides of three reactions. With respect to the three transition states, all of the breaking C−H

Table 1. Calculated and Experimental Frequencies (in cm^{-1}) of the Reactants, Complexes, Products and Transition States at the MP2/6-311G(d, p) Level

	MP2/6-311G(d, p)	exptl.
CH_3F	1106,1224,1224,1519,1519,1537,3088,3186,3186	1049,1182,1182,1464,1464,1467,2965,3006,3006[a]
CH_3Cl	784,1064,1064,1441,1496,1496,3119,3227,3227	732,1017,1017,1355,1455,1455,2968,3054,3054[b]
CH_3Br	648,990,990,1381,1496,1496,3121,3237,3237	611,955,955,1306,1443,1443,2935,3056,3056[c]
HF	4252	4138[d]
CH_2F	713,1206,1212,1520,3193,3351	
CH_2Cl	161,879,1046,1474,3239,3394	
CH_2Br	98,732,967,1438,3232,3390	
CR_1	10,18,20,1107,1224,1224,1519,1519,1536,3088,3186,3187	
CP_1	60,91,116,288,315,779,1209,1212,1516,3193,3350,4195	
CR_2	19,67,87,783,1065,1069,1442,1498,1500,3122,3226,3237	
CP_2	36,75,112,282,285,561,880,1051,1471,3222,3371,4200	
CR_3	27,28,78,647,991,994,1379,1495,1498,3125,3238,3246	
CP_3	30,74,108,279,289,559,735,972,1437,3214,3364,4196	
TS1	866i,103,144,853,1146,1207,1307,1388,1523,1864,3133,3224	
TS2	954i,77,149,780,835,1050,1198,1349,1466,1746,3162,3252	
TS3	1028i,81,164,603,724,981,1171,1346,1444,1784,3167,3260	

[a] From ref 27. [b] From ref 28. [c] From ref 31. [d] From ref 29.

Table 2. Enthalpies (in kcal mol^{-1}) and Barrier Heights (in kcal mol^{-1}) at MP2/6-311G(d, p) and CCSD(T)/6-311++G(3df, 2pd)//MP2/6-311G(d, p) Levels and Available Experimental Values

	$CH_3F + F \rightarrow HF + CH_2F$		$CH_3Cl + F \rightarrow HF + CH_2Cl$		$CH_3Br + F \rightarrow HF + CH_2Br$	
levels	ΔH_{298}^0	ΔE(0 K)	ΔH_{298}^0	ΔE(0 K)	ΔH_{298}^0	ΔE(0 K)
MP2	−32.58	3.48	−32.71	3.86	−31.75	3.90
CCSD(T)	−34.80	−4.02 (−2.27)[b] [−0.81][c]	−36.73	−5.12 (−3.18)[b]	−35.58	−5.16 (−3.30)[b]
exptl.[a]	−36.14 ± 3.3		−35.54 ± 2.3		−35.64 ± 2.3	

[a] From ref 32. [b] The values in the parentheses including BSSE corrections. [c] The values in the square bracket obtained at the CCSD(T)**/**6-311++G(3df, 2pd**)//**QCISD**/**6-311G**(**d, p) level with BSSE correction.

bonds are elongated by 4.6% compared to the C−H equilibrium bond length in isolated CH_3F, CH_3Cl, and CH_3Br, respectively; and the forming H−F bond is elongated by 55, 53 and 53% with respect to the H−F equilibrium bond length in isolated HF, respectively. The elongation of the forming bond is greater than that of the breaking bond, indicating that the three TSs are reactant-like, i.e., all these reactions proceed via "early" transition states. This rather early character in these transition states is in accordance with the low barrier heights and the exothermicity of these reactions, in keeping with Hammond's postulate.[30]

The harmonic vibrational frequencies are calculated at the same level of theory to characterize the nature of each critical point and to make zero-point energy (ZPE) corrections. Table 1 lists the harmonic vibrational frequencies of all the stationary points along with the available experimental data.[27−29,31] Our calculated frequencies are in good agreement with the experimental values, with the largest deviation within 9%. The number of imaginary frequencies (0 or 1) indicates whether a minimum or a transition state has been located. All of the complexes have only real frequencies. The transition state is confirmed by normal-mode analysis to have only one imaginary frequency, which takes the values of 866*i*, 954*i*, and 1028*i* cm^{-1}, respectively.

The reaction enthalpies (ΔH_{298}°) and classical barrier heights (ΔE(0K)) calculated at the MP2/6-311G(d, p) and CCSD(T)/6-311++G(3df, 2pd)//MP2 levels with ZPE and BSSE corrections are listed in Table 2. The calculated enthalpies of −34.80, −36.73, and −35.58 kcal mol^{-1} for the series of reactions at the higher level are in good agreement with the experimental values of −36.14 ± 3.3, −35.54 ± 2.3, and −35.64 ± 2.3 kcal mol^{-1}, respectively, which is derived from the experimental standard heats of formation (CH_3F, −56 ± 1 kcal mol^{-1}; CH_3Cl −19.6 kcal mol^{-1}; CH_3Br, −8.5 kcal mol^{-1}; CH_2F, −8 ± 2 kcal mol^{-1}; CH_2Cl, 29 ± 2 kcal mol^{-1}; CH_2Br, 40 ± 2 kcal mol^{-1}; HF, −65.14 ± 0.2 kcal mol^{-1}; F, 19.0 ± 0.1 kcal mol^{-1}).[32] For reactions $CH_3F + F \rightarrow CH_2F + HF$, $CH_3Cl + F \rightarrow CH_2Cl + HF$, and $CH_3Br + F \rightarrow CH_2Br + HF$, the complexes CR_1, CR_2, and CR_3 are first formed with relative energies being −0.38, −0.32, and −1.52 kcal mol^{-1} below the reactants of $CH_3F + F$, $CH_3Cl + F$, and $CH_3Br + F$ at the CCSD(T)//MP2 level with ZPE corrections, respectively. Then starting from the complex, each of the reaction passes through a reactant-like transition state to form another complex with relative energies of 0.70, 0.19, and 0.23 kcal mol^{-1} below the products of $CH_2F + HF$, $CH_2Cl + HF$, and $CH_2Br + HF$, respectively. It is seen that the energies of the complexes are very close to those of the reactants or products, so one question arises: do these complexes really exist or is it an artifact due to the theoretical methods? To test the stability of the complexes, the basis set superposition error (BSSE) correction is estimated using the counterpoise method. At the CCSD(T)/6-311++G(3df, 2pd) level, we obtain BSSEs of 0.28, 0.38, and 0.48 kcal mol^{-1} for CR_1, CR_2, and CR_3, respectively. Thus, the BSSE-corrected energies for three complexes are −0.11, 0.06, and −1.04 kcal mol^{-1}, respectively. Similarly, the corresponding values for complexes

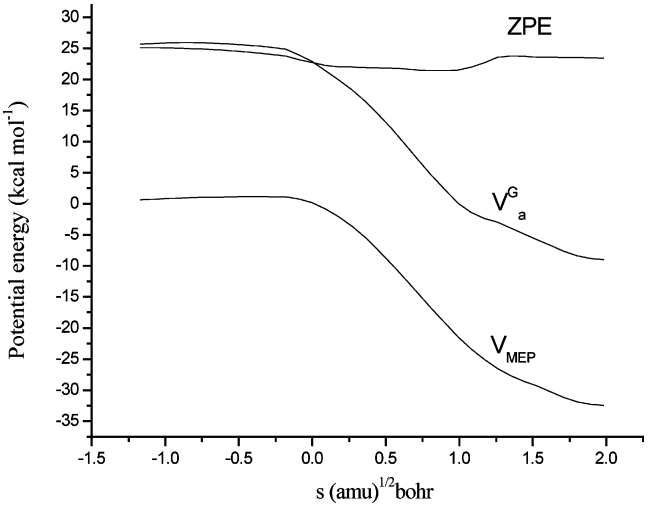

Figure 2. Classical potential energy curve (V_{MEP}), ground-state vibrationally adiabatic energy curve (V_a^G), and zero-point energy curve (ZPE) as functions of s (amu)$^{1/2}$ bohr at the CCSD(T)/6-311++G(3df, 2pd)//MP2/6-311G(d, p) level with BSSE correction for the $CH_3F + F \rightarrow CH_2F + HF$.

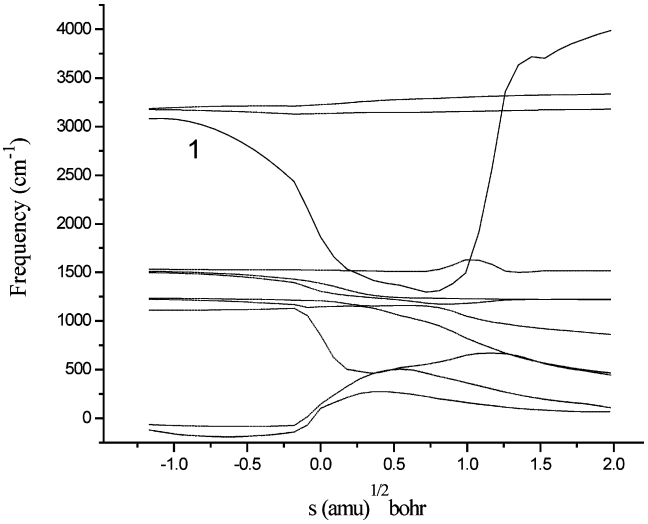

Figure 3. Changes in the generalized normal-mode vibrational frequencies as functions of s (amu)$^{1/2}$ bohr at the MP2/6-311G(d, p) level for the $CH_3F + F \rightarrow CH_2F + HF$.

CP_1, CP_2, and CP_3 are -0.22, 0.30, and 0.25 kcal mol^{-1} relative to the products, respectively. It can be found that complexes CR_2, CP_2 and CP_3 disappear when BSSE correction is included. With respect to the barrier heights, the calculated results of three reactions obtained at the MP2 level are 3.48, 3.86, and 3.90 kcal mol^{-1}, respectively, while at the CCSD(T)//MP2 level, the corresponding values are 4.02, 5.12, and 5.16 kcal mol^{-1} below the reactants, respectively. When the BSSE is considered, as calculated in the complexes, the barrier heights are -2.27, -3.18, and -3.30 kcal mol^{-1} at CCSD(T)//MP2 level, respectively. Moreover, for comparison we performed the optimization calculation for reaction R1 at higher level of electron correlation QCISD/6-311G(d, p) with the single-point energies for the stationary points at the same CCSD(T)/6-311++G(3df, 2pd) level (Table 2). The calculated enthalpies (ΔH_{298}°) value is -34.81 kcal mol^{-1} at the CCSD(T)//QCISD level, which is in excellent agreement with both the experimental results and the theoretical ones obtained at the CCSD(T)//MP2 level. The barrier height of reaction R1 is -0.81 kcal mol^{-1} at CCSD(T)//QCISD level with ZPE and BSSE corrections. It can be found that the classical barrier heights obtained at two higher levels are very closed except that the value calculated at CCSD(T)//QCISD level is slightly higher than that obtained at CCSD(T)//MP2 level.

The potential profile is further refined by performing a series of single point calculations at the CCSD(T)/6-311++G(3df, 2pd)//MP2 level including the BSSE correction. The classical potential energy curve ($V_{MEP}(s)$), the vibrationally adiabatic ground-state potential energy curve ($V_a^G(s)$), and the zero-point energy (ZPE) curve of the reaction R1 as a function of the intrinsic reaction coordinate (s) are plotted in Figure 2, where $V_a^G(s) = V_{MEP}(s) + \text{ZPE}(s)$. As can be seen, the V_{MEP} and V_a^G curves are similar in shape, and the ZPE is practically constant as s varies with only a gentle drop near the saddle point. It should be noted that the locations of maximum on the $V_a^G(s)$ and $V_{MEP}(s)$ energy curves shift in the s direction toward the reactants and the maximum of the two curves are slightly higher than the reactants. This is the case that the saddle-point position of the dual-level is generally shifted. The same conclusion can be drawn from the other two reactions.

The variations of the generalized normal-mode vibrational frequencies along the MEP of reaction R1 is shown in Figure 3, and the similar figures for the reactions R2 and R3 are omitted for simplicity. In the negative limit of s, the frequencies are associated with the reactants $F + CH_3F$, and in the product region the frequencies correspond to the products $HF + CH_2F$. In Figure 3, all of the frequencies except for mode 1 do not change significantly on going from the reactants to the products. The "reactive mode" 1 relating to the breaking/forming bonds has a significant change from $s = 0$ to 1.0 (amu)$^{1/2}$ bohr on the MEP. These drops should cause considerable falls in the ZPE near the saddle point. On the other hand, the two lowest harmonic frequencies corresponding to free rotations and translations of the reactants evolve into vibrations and they present a maximum near the saddle point. The behavior of these transitional modes partially compensated the fall in the ZPE caused by the reactive mode, thus the ZPE shows small variations with s.

2. Dynamics Calculation. Dual-level (X//Y)[16−18] direct dynamics calculations are carried out for the three reactions using the variational transition-state theory. The BSSE-corrected and noncorrected PES information for each reaction obtained at the CCSD(T)/6-311++G(3df, 2pd)//MP2/6-311G(d, p) level is put into Polyrate 8.4.1 program[19] to calculate the VTST[20,21] rate constants over the temperature range from 189 to 2000 K. The forward rate constants are calculated by canonical variational transition-state theory (CVT)[24] with the small-curvature tunneling (SCT)[25] method.

The theoretical rate constants based on the BSSE-corrected PES and the available experimental values are shown in Figure 4a-c. For the reaction of $CH_3F + F$ (see Figure 4a), our calculated results agree well with the experimental values[5−9] except the results reported by Nielsen et. al. (8.8×10^{-11} cm^3 molecule^{-1} s^{-1})[4] and the values given by Kowalczyk et. al. ($(6.59 \pm 1.51) \times 10^{-12}$ cm^3 molecule^{-1}

Table 3. Calculated Rate Constants (in cm^3 $molecule^{-1}$ s^{-1}) for the Reaction (a) $CH_3F + F \rightarrow CH_2F + HF$, (b) $CH_3Cl + F \rightarrow CH_2Cl + HF$, (c) $CH_3Br + F \rightarrow CH_2Br + HF$ in the Temperature Range from 189 to 2000 K and Available Experimental Values

T (K)	$k_1(10^{11})$	$k_{exptl.}(10^{11})$	$k_2(10^{11})$	$k_{exptl.}(10^{11})$	$k_3(10^{11})$	$k_{exptl.}(10^{11})$
189	0.90	1.30 ± 0.10[a]	1.23		1.45	
219	1.10	1.76 ± 0.20[a]	1.43		1.70	
225	1.13		1.47		1.75	
251	1.31	2.17 ± 0.20[a]	1.61		1.98	
275	1.48		1.74		2.19	
295	1.62	3.7 ± 0.8[b]	1.88	2.4 ± 0.5[h]	2.36	6.1 ± 0.7[j]
				3.3 ± 0.7[b]		4.5 ± 0.9[k]
						3.0 ± 0.7[b]
296	1.63		1.89		2.37	4.5 ± 0.2[l]
298	1.64	8.8[c]	1.90	2.4 ± 0.7[i]	2.39	
		3.6 ± 0.2[d]				
		3.0[e]				
		2.8 ± 0.6[f]				
		2.76 ± 0.20[a]				
		0.66 ± 0.15[g]				
300	1.66		1.92		2.41	
400	2.46		2.69		3.31	
500	3.41		3.60		4.35	
600	4.56		4.66		5.65	
900	8.94		8.73		10.5	
1000	10.6		10.4		12.5	
1200	14.2		13.9		16.8	
1500	20.6		19.6		24.0	
2000	33.0		31.3		37.8	

[a] From ref 9. [b] From ref 7. [c] From ref 4. [d] From ref 5. [e] From ref 6. [f] From ref 8. [g] From ref 10. [h] From ref 12. [i] From ref 11. [j] From ref 13. [k] From ref 14. [l] From ref 15.

s^{-1}).[10] The deviation remains within a factor of about 1.4−2.0. Moreover, the Arrhenius expression of $k_1 = 4.71 \times 10^{-11}\exp(-317.2/T)$ cm^3 $molecule^{-1}$ s^{-1} fitted by the CVT/SCT rate constant in the temperature range 189−298 K is in good accord with that reported by Persky,[9] $k = (1.03 \pm 0.13) \times 10^{-10}\exp[-(390 \pm 60)/T]$ cm^3 $molecule^{-1}$ s^{-1}. As to the hydrogen abstraction reaction of $CH_3Cl + F$ (see Figure 4b), the agreement between the theoretical rate constants and experimental ones[7,11−12] is considerably good, where the factor of deviation is only 1.0−1.4. As can be seen from Figure 4c the experimental rate constant[7,13−15] for $CH_3Br + F$ reaction determined by Iyer and Rowland[13] is slightly higher than the other data, and our calculated result is in better agreement with the latter. In addition, the theoretical rate constants calculated on the potential energy surface without a BSSE correction are shown in the Supporting Information. It is obvious that when the BSSE correction is included in the classical barrier heights increase, as a result, the values of rate constants are lowered about 1−3 times in the lower temperature range. However, the discrepancy between them becomes smaller and almost disappears with the temperature increasing.

To reflect the effect of halogen substitution on the reactivity of the C−H bond, Arrhenius expressions are fitted based on the calculated rate constants of the three reactions in the temperature range 225−600 K. The preexponential factors (A) and activation energies (E_a) are given in Table 4. It is shown that there is a slight influence on both A and E_a for the halogen substitutions from F to Br. The activation energies decrease in the order of R1 (1.00) > R2 (0.84) > R3 (0.83), but the discrepancy among them is considerably small. Thus, it results in a small decrease of the rate constant from R3 to R1, i.e., $k_3 > k_2 > k_1$. In addition, the activation energies of these reactions are correlated with the hardness of the halomethane molecules.[33] The hardness η is defined as $\eta = (IE-EA)/2$, where IE and EA are the first vertical ionization energy and electron affinity of the molecule, respectively. The values of the hardness η of CH_3F, CH_3Cl, and CH_3Br are 164.6, 139.4, and 130.6 kcal mol^{-1} at the CCSD(T)//MP2 level, respectively, decreasing in the order of $CH_3F > CH_3Cl > CH_3Br$. Clearly, if the systems become softer, charge transfer between the reactants will be easier and the reaction will become more activity.

Owing to the good agreement between the theoretical and experimental values, it is reasonable to believe that our calculated results will provide a good estimate for the kinetics of the reactions in the high-temperature range. Note that although there have been some kinetic studies performed on the title reactions, most of the rate constants are measured around room temperature. Therefore, for convenience of future experimental measurements, the three-parameter fits for the CVT rate constants for the title reactions within 189−2000 K give the expressions as follows (in cm^3 $molecule^{-1}$ s^{-1}):

$$k_1 = 5.38 \times 10^{-16} T^{1.75} \exp(109.7/T)$$

$$k_2 = 3.81 \times 10^{-16} T^{1.78} \exp(202.2/T)$$

$$k_3 = 7.06 \times 10^{-16} T^{1.72} \exp(176.3/T)$$

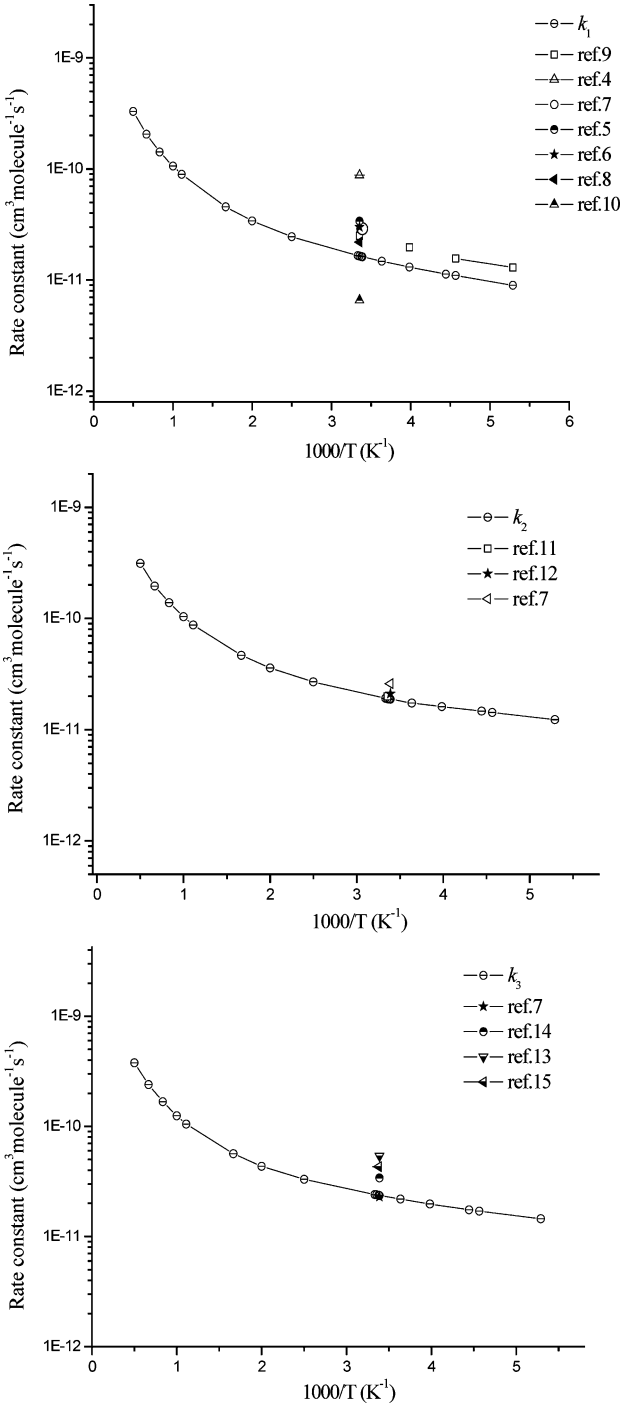

Figure 4. Plot of the CVT/SCT rate constants calculated at the CCSD(T)/6-311++G(3df, 2pd)//MP2/6-311G(d, p) level with BSSE correction and the available experimental values versus 1000/*T* between 189 and 2000 K for the (a) $CH_3F + F \rightarrow CH_2F + HF$, (b) $CH_3Cl + F \rightarrow CH_2Cl + HF$, (c) $CH_3Br + F \rightarrow CH_2Br + HF$.

Table 4. Arrhenius Parameters[a] for the Title Reactions

reaction	A ($cm^3\ s^{-1}$)	E_a(kcal mol^{-1})
$F + CH_3F$	9.27×10^{-11}	1.00
$F + CH_3Cl$	8.26×10^{-11}	0.84
$F + CH_3Br$	1.01×10^{-10}	0.83

[a] In the temperature range of 225−600 K.

Conclusion

In the present paper, we employ an ab initio direct dynamic method to study three hydrogen abstraction reactions of CH_3X (X=F, Cl, and Br) with F atoms. The potential energy surface information is obtained at the MP2/6-311G(d, p) level and higher level energies of the stationary points are calculated at the higher CCSD(T)/6-311++G(3df, 2pd) level with ZPE and BSSE corrections. The rate constant calculations are carried out using the variational transition state theory (VTST) at the CCSD(T)//MP2 level over a wide temperature range of 189−2000 K. The correlation among the activation energies, the rate constants, and the hardness of the halomethane molecules is discussed. For three reactions the calculated rate constants decrease in the order of $k_3 > k_2 > k_1$, which is just opposite of the orders of the theoretical activation energies and the hardness of halomethane molecules. Theoretical rate constants show good agreement with the available experimental values. The three-parameter expressions (in cm^3 $molecule^{-1}$ s^{-1}) for three reactions within 189−2000 K are $k_1 = 5.38 \times 10^{-16}T^{1.75}\exp(109.7/T)$, $k_2 = 3.81 \times 10^{-16}T^{1.78}\exp(202.2/T)$, and $k_3 = 7.06 \times 10^{-16}T^{1.72}\exp(176.3/T)$ cm^3 $molecule^{-1}$ s^{-1}. We hope the theoretical results may be useful for estimating the kinetics of the reactions over a wide temperature range where no experimental data are available.

Acknowledgment. We thank Professor Donald G. Truhlar for providing of the POLYRATE 8.4.1 program. This work was supported by the National Natural Science Foundation of China (20333050, 20303007), the Doctor Foundation by the Ministry of Education, the Foundation for University Key Teacher by the Ministry of Education, the Key Subject of Science and Technology by the Ministry of Education of China, and the Innovational Foundation by Jilin University.

Supporting Information Available: Plot of the CVT/SCT rate constants (Figure S1). This material is available free of charge via the Internet at http://pubs.acs.org.

References

(1) Atkinson, R. Kinetics and mechanisms of the gas-phase reactions of the hydroxyl radical with organic compounds under atmospheric conditions. *Chem. Rev.* **1986**, *86*, 69−201.

(2) Paddison, S. J.; Tschuikow-Roux, E. Structures, Vibrational Frequencies, Thermodynamic Properties, and Bond Dissociation Energies of the Bromomethanes and Bromomethyl Radicals: an Ab Initio Study. *J. Phys. Chem. A* **1998**, *102*, 6191−6199.

(3) Bilde, M.; Wallington, T. J.; Ferronato, C.; Orlando, J. J.; Tyndall, G. S.; Estupiñan, E.; Haberkorn, S. Atmospheric Chemistry of CH_2BrCl, $CHBrCl_2$, $CHBr_2Cl$, $CF_3CHBrCl$, and CBr_2Cl_2. *J. Phys. Chem. A* **1998**, *102*, 1976−1986.

(4) Pollock, T. L.; Jones, W. E. Gas-phase reactions of fluorine atoms. *Can. J. Chem.* **1973**, *51*, 2041−2046.

(5) Manning, R. G.; Grant, E. R.; Merrill, J. C.; Parks, N. J.; Root, J. W. Hydrogen abstraction by fluorine atoms under conditions of thermal initiation: Hydrocarbons and fluorinated hydrocarbons. *Int. J. Chem. Kinet.* **1975**, *7*, 39−44.

(6) Smith, D. J.; Setser, D. W.; Kim, K. C.; Bogan, D. J. HF infrared chemiluminescence. Relative rate constants for hydrogen abstraction from hydrocarbons, substituted methanes, and inorganic hydrides. *J. Phys. Chem.* **1977**, *81*, 898−905.

(7) Wallington, T. J.; Hurley, M. D.; Shi, J.; Maricq, M. M.; Sehested, J.; Nielsen, O. J.; Ellermann, T. A kinetic study of the reaction of fluorine atoms with CH_3F, CH_3Cl, CH_3Br, CF_2H_2, CO, CF_3H, CF_3CHCl_2, CF_3CH_2F, CHF_2CHF_2, CF_2ClCH_3, CHF_2CH_3, and CF_3CF_2H at 295 ± 2 K. *Int. J. Chem. Kinet.* **1993**, *25*, 651−665.

(8) Moore, C.; Smith, I. W. M. Rate constants for the reactions of fluorine atoms with alkanes and hydrofluorocarbons at room temperature. *J. Chem. Soc., Faraday Trans.* **1995**, *91*, 3041−3044.

(9) Persky, A. The temperature dependence of the rate constants for the reactions F + CH_3F and F + CH_2F_2. *Chem. Phys. Lett.* **2003**, *376*, 181−187.

(10) Kowalczyk, J.; Jowko, A.; Symanowicz, M. Kinetics of radical reactions in Freons. *J. Radioanal. Nucl. Chem.* **1998**, *232*, 75−78.

(11) Clyne, M. A. A.; McKenney, D. J.; Walker, R. F. Reaction kinetics of ground-state fluorine, F(^{2}P), atoms. I. Measurement of fluorine atom concentrations and the rates of reactions F + CHF_3 and F + Cl_2 using mass spectrometry. *Can. J. Chem.* **1973**, *51*, 3596−3604.

(12) Wickramaaratchi, M. A.; Setser, D. W.; Hildebrandt, H.; Korbitzer, B.; Heydtmann, H. Evaluation of HF product distributions deduced from infrared chemiluminescence. II. F atoms reactions. *Chem. Phys.* **1985**, *94*, 109−129.

(13) Iyer, R. S.; Rowland, F. S. Atom-transfer reaction rates for thermal fluorine atoms with CH_3X and CF_3X (X = Br, I). *J. Phys. Chem.* **1981**, *85*, 2493−2497.

(14) Nielsen, O. J.; Munk, J.; Locke, G.; Wallington, T. J. Ultraviolet absorption spectra and kinetics of the self-reaction of bromomethyl and peroxybromomethyl radicals in the gas phase at 298 K. *J. Phys. Chem.* **1991**, *95*, 8714−8719.

(15) Sehested, J.; Bilde, M.; Mogelberg, T.; Wallington, T. J.; Nielsen, O. J. Kinetics and mechanism of the reaction of F atoms with CH_3Br. *J. Phys. Chem.* **1996**, *100*, 10989−10998.

(16) Truhlar, D. G. In *The Reaction Path in Chemistry: Current Approaches and Perspectives;* Heidrich, D. Ed.; Kluwer: Dordrecht The Netherlands, 1995, p 229.

(17) Truhlar, D. G.; Garrent, B. C.; Klippenstein, S. J. Current Status of Transition-State Theory. *J. Phys. Chem.* **1996**, *100*, 12771−12800.

(18) Hu, W. P.; Truhlar, D. G. Factors Affecting Competitive Ion−Molecule Reactions: ClO^- + C_2H_5Cl and C_2D_5Cl via E2 and S_N2 Channels. *J. Am. Chem. Soc.* **1996**, *118*, 860−869.

(19) Chuang, Y.-Y.; Corchado, J. C.; Fast, P. L.; Villa, J.; Hu, W.-P.; liu, Y.-P.; Lynch, G. C.; Jackels, C. F.; Nguyen, K. A.; Gu, M. Z.; Rossi, I.; Coitino, E. L.; Clayton, S.; Melissas, V. S.; Lynch, B. J.; Steckler, R.; Garrett, B. C.; Isaacson, A. D.; Truhlar, D. G. *Polyrate, version 8.4.1*, University of Minnnesota, Minneapolis, MN, 2000.

(20) Truhlar, D. G.; Garrett, B. C. Variational transition-state theory. *Acc. Chem. Res.* **1980**, *13*, 440−448.

(21) Truhlar, D. G.; Isaacson, A. D.; Garrett, B. C. In *The Theory of Chemical Reaction Dynamics*; Baer, M., Ed.; CRC Press: Boca Raton, FL, 1985, p 65.

(22) Frisch, M. J.; Truck, G. W.; Schlegel, H. B.; Scuseria, G. E.; Robb, M. A.; Cheeseman, J. R.; Zakrzewski, V. G.; Montgomery, J. A.; Jr.; Stratmann, R. E.; Burant, J. C.; Dapprich, S.; Millam, J. M.; Daniels, A. D.; Kudin, K. N.; Strain, M. C.; Farkas, O.; Tomasi, J.; Barone, V.; Cossi, M.; Cammi, R.; Mennucci, B.; Pomelli, C.; Adamo, C.; Clifford, S.; Ochterski, J.; Petersson, G. A.; Ayala, P. Y.; Cui, Q.; Morokuma, K.; Malick, D. K.; Rabuck, A. D.; Raghavachari, K.; Foresman, J. B.; Cioslowski, J.; Ortiz, J. V.; Boboul, A. G.; Stefnov, B. B.; Liu, G.; Liaschenko, A.; Piskorz, P.; Komaromi, L.; Gomperts, R.; Martin, R. L.; Fox, D. J.; Keith, T.; Al-Laham, M. A.; Peng, C. Y.; Nanayakkara, A.; Gonzalez, C.; Challacombe, M.; Gill, P. M. W.; Johnson, B.; Chen, W.; Wong, M. W.; Andres, J. L.; Gonzalez, C.; Head-Gordon, M.; Replogle E. S.; Pople, J. A. *Gaussian 98*, revision X.; Gaussian Inc.: Pittsburgh, PA, 1998.

(23) Boys, S. F.; Bernardi, F. The calculation of small molecular interactions by the differences of separate total energies. Some procedures with reduced errors. *Mol. Phy.* **1970**, *19*, 553−566.

(24) Garrett, B. C.; Truhlar, D. G. Criterion of minimum state density in the transition state theory of bimolecular reactions. *J. Chem. Phys.* **1979**, *70*, 1593−1598.

(25) Liu, Y.-P.; Lynch, G. C.; Truong, T. N.; Lu, D.-h.; Truhlar, D. G.; Garrett, B. C. Molecular modeling of the kinetic isotope effect for the [1,5]-sigmatropic rearrangement of *cis*-1, 3-pentadiene. *J. Am. Chem. Soc.* **1993**, *115*, 2408−2415.

(26) Corchado, J. C.; Truhlar, D. G.; Espinosa-Garcia, J. Potential energy surface, thermal, and state-selected rate coefficients, and kinetic isotope effects for Cl + CH_4 →HCl + CH_3. *J. Chem. Phys.* **2000**, *112*, 9375−9388.

(27) JANAF Themochemical Tables: National Standard Reference Data Aeries; National Bureau of Standards: Washington, DC, 1986; Vol. 37, 2nd ed.

(28) Kuchitsu, K. in Structure of Free Polyatomic Molecules Basic Data (Springer, Sakado), 1998, Vol. 104, p 94.

(29) Linstrom, P. J.; Mallard, W. G.NIST Chemistry Webbook, http://webbook.nist.gov/chemistry/ 1998.

(30) Hammond, G. S. A Correlation of Reaction Rates. *J. Am. Chem. Soc.* **1955**, *77*, 334−338.

(31) Lide, D. R. In CRC Handbook of Chemistry and Physics, 73rd ed. (CRC, Boca Raton, 1992).

(32) DeMore, W. B.; Sander, S. P.; Golden, S. P.; Howard, C. J.; Golden, D. M.; Kolb, C. E.; Hampson, R. F.; Molina, M. J. Chemical Kinetics and Photochemical Data for Use in Stratospheric Modeling, 1997.

(33) Chandra, A. K.; Uchimaru, T.; Sugie, M.; Sekiya, A. Correlation between hardness and activation energies for reactions of OH radical with halomethanes. *Chem. Phys. Lett.* **2000**, *318*, 69−71.

CT049932+